Plasticenta: First evidence of microplastics in human placenta

Antonio Ragusa [a], Alessandro Svelato [a,*], Criselda Santacroce [b], Piera Catalano [b], Valentina Notarstefano [c], Oliana Carnevali [c], Fabrizio Papa [b], Mauro Ciro Antonio Rongioletti [b], Federico Baiocco [a], Simonetta Draghi [a], Elisabetta D'Amore [a], Denise Rinaldo [d], Maria Matta [e], Elisabetta Giorgini [c]

[a] Department of Obstetrics and Gynecology, San Giovanni Calibita Fatebenefratelli Hospital, Isola Tiberina, Via di Ponte Quattro Capi, 39, 00186 Rome, Italy
[b] Department of Pathological Anatomy, San Giovanni Calibita Fatebenefratelli Hospital, Isola Tiberina, Via di Ponte Quattro Capi, 39, 00186 Roma, Italy
[c] Department of Life and Environmental Sciences, Università Politecnica delle Marche, via Brecce Bianche, 60131 Ancona, Italy
[d] Department of Obstetrics and Gynecology, ASST Bergamo Est, Bolognini Hospital, Seriate, Via Paderno, 21, 24068 Bergamo, Italy
[e] Harvey Medical and Surgery Course, University of Pavia, Corso Strada Nuova 65, 27100 Pavia, Italy

ARTICLE INFO

ABSTRACT

Microplastics are particles smaller than five millimeters deriving from the degradation of plastic objects present in the environment. Microplastics can move from the environment to living organisms, including mammals. In this study, six human placentas, collected from consenting women with physiological pregnancies, were analyzed by Raman Microspectroscopy to evaluate the presence of microplastics. In total, 12 microplastic fragments (ranging from 5 to 10 μm in size), with spheric or irregular shape were found in 4 placentas (5 in the fetal side, 4 in the maternal side and 3 in the chorioamniotic membranes); all microplastics particles were characterized in terms of morphology and chemical composition. All of them were pigmented; three were identified as stained polypropylene a thermoplastic polymer, while for the other nine it was possible to identify only the pigments, which were all used for man-made coatings, paints, adhesives, plasters, finger paints, polymers and cosmetics and personal care products.

1. Introduction

In the last century, the global production of plastics has reached 320 million tons (Mt) per year, and over 40% is used as single-use packaging, hence producing plastic waste. In Europe, plastic production reached the 58 millions of tons in 2014 (PlasticsEurope, 2016). The degradation that plastics undergo when released into the environment is a serious issue. Atmospheric agents, such as waves, abrasion, ultraviolet radiation and photo-oxidation in combination with bacteria degrade plastic fragments into micro and nanosized particles. Most of the seabed all over the world and in the Mediterranean Sea in particular, is made of plastic, resulting from the waste collected on the coasts and in the sea (de Souza Machado et al., 2018). Microplastics (MPs) are defined as particles less than 5 mm in size (Hartmann et al., 2019). MPs do not derive only from larger pieces fragmentation but are also produced in these dimensions for commercial uses. Furthermore, there are several reports of MPs in food (Barboza et al., 2018), and in particular in seafood, sea salt (Karami et al., 2017b; Kosuth et al., 2018), and in drinking water (Schymanski et al., 2018). Microplastics have also been detected in the gastrointestinal tract of marine animals (Deng et al., 2017; Reineke et al., 2013), and also human intestine (Schwabl et al., 2019). Inside tissues, MPs are considered as foreign bodies by the host organism and, as such, trigger local immunoreactions. Furthermore, MPs can act as carriers for other chemicals, such as environmental pollutants and plastic additives, which may be released and are known for their harmful effects (EFSA Panel on Contaminants in the Food Chain (CONTAM), 2016; Wright and Kelly, 2017).

In this study, for the first time, several microplastic fragments were detected by Raman Microspectroscopy in human placenta samples collected from six consenting patients with uneventful pregnancies. Raman Microspectroscopy is a well-assessed vibrational technique, widely and successfully applied in the biomedical field, to characterize both biological samples (Notarstefano et al., 2020, 2019), and to detect the occurrence of microplastics and microparticles in general (Käppler et al., 2016; Ribeiro-Claro et al., 2017). Placenta finely regulates foetal to maternal environment and, indirectly, to the external one, acting as a

---

crucial interface via different complex mechanisms (PrabhuDas et al., 2015). The potential presence of man-made MPs in this organ may harm the delicate response of differentiation between self and non-self (Nancy et al., 2012) with a series of related consequences on embryo development that need to be defined.

2. Materials and methods

2.1. Experimental design

This was a pilot observational descriptive preclinical study, with a prospective and unicentric open cohort. It was approved by the Ethical Committee Lazio 1 (Protocol N. 352/CE Lazio 1; March 31th, 2020), and it was carried out in full accordance with ethical principles, including The Code of Ethics of the World Medical Association (Declaration of Helsinki) for experiments involving humans. To participate to this study, six selected consenting patients signed an informed consent, which included donation of placentas.

To prevent plastic contamination, a plastic-free protocol was adopted during the entire experiment. Obstetricians and midwives used cotton gloves to assist women in labour. In the delivery room, only cotton towels were used to cover patients' beds; graduate bags to estimate postpartum blood loss were not used during delivery, but they were brought in the delivery room only after birth, when umbilical cord was already clamped and cut with metal clippers, avoiding contact with plastic material. Pathologists wore cotton gloves and used metal scalpels.

The schematic illustration for the overall concept and experimental procedure is reported in Fig. 1.

2.2. Enrolment of patients and placentas collection

All recruited women were healthy and have a vaginal delivery at term of pregnancy at the Department of Obstetrics and Gynaecology of San Giovanni Calibita Fatebenefratelli Hospital, Isola Tiberina, Roma (Italy). They were selected according to the following exclusion criteria: diagnosis of gastrointestinal disease, such as ulcerative colitis, or Crohn's disease, cancer, organ transplantation, HIV (Human Immuno-deficiency Virus), or other severe pathologies; alcohol abuse (defined as a >10 score in the Alcohol Use Disorders Identification Test); cigarette smoking; peculiar diets prescribed for particular medical conditions (four weeks before delivery); diarrhoea or constipation (two weeks before delivery); antibiotics intake (two weeks before delivery); assumption of drugs affecting intestinal reabsorption, such as activated charcoal, or cholestyramine (two weeks before delivery); invasive or abrasive dental treatments (two weeks before delivery); participation to
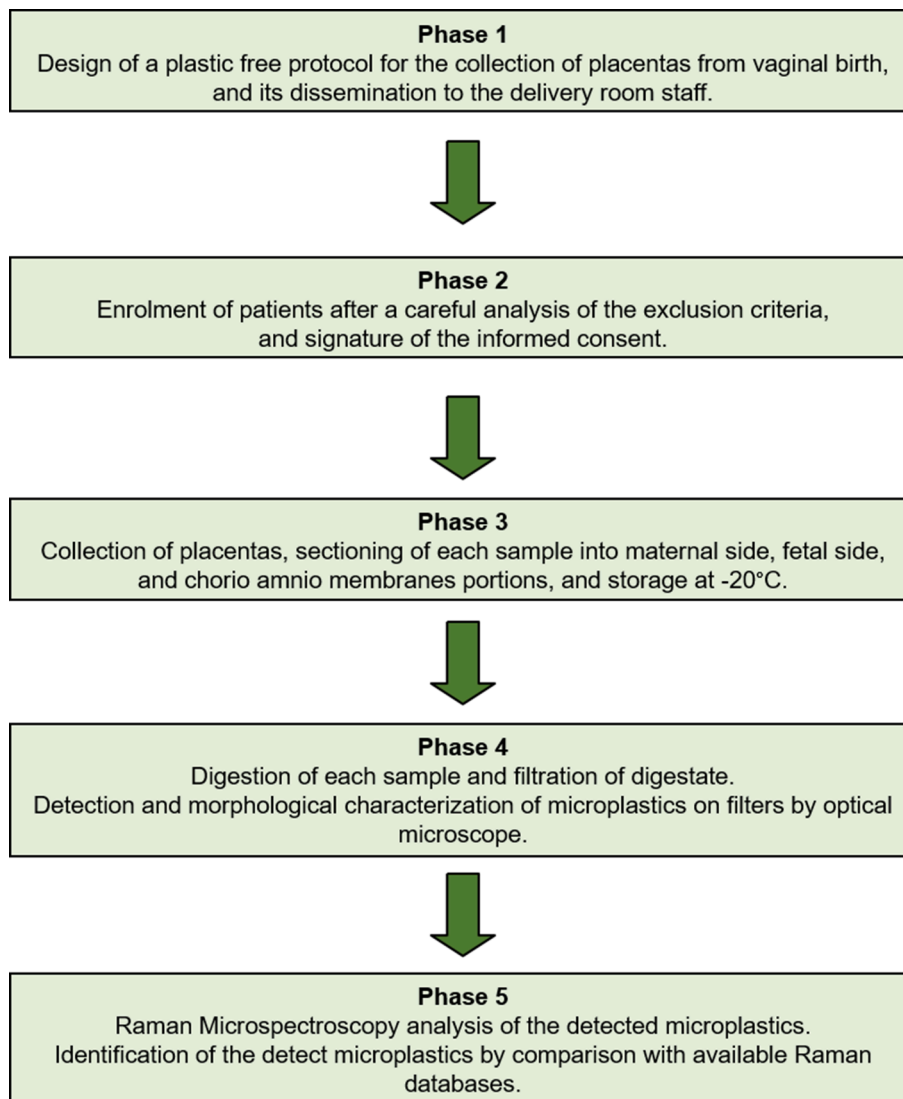
Phase 1
Design of a plastic free protocol for the collection of placentas from vaginal birth, and its dissemination to the delivery room staff.

⬇

Phase 2
Enrolment of patients after a careful analysis of the exclusion criteria, and signature of the informed consent.

⬇

Phase 3
Collection of placentas, sectioning of each sample into maternal side, fetal side, and chorio amnio membranes portions, and storage at -20°C.

⬇

Phase 4
Digestion of each sample and filtration of digestate.
Detection and morphological characterization of microplastics on filters by optical microscope.

⬇

Phase 5
Raman Microspectroscopy analysis of the detected microplastics.
Identification of the detect microplastics by comparison with available Raman databases.

Fig. 1. Schematic illustration for the overall concept and experimental procedure followed in the study.

a clinical study (four weeks before delivery). Women were also asked to fill a questionnaire to record their food consumption (omnivorous, vegetarian, vegan, with no diet restriction) the week before delivery and the use of toothpastes and cosmetics containing MPs or synthetic polymers.

After birth, placentas were deposed onto a metal container and immediately sectioned in portions (mean weight: 23.3 ± 5.7 g) taken from maternal side, foetal side, and chorioamniotic membranes. All samples were strictly anonymous; they were labelled with number codes and stored in glass bottles with metal lids at −20 °C with no further treatment.

2.3. Digestion of placenta samples

The digestion of placenta samples was performed at the Laboratory of Vibrational Spectroscopy, Department of Life and Environmental Sciences, Università Politecnica delle Marche (Ancona, Italy), modifying as follows the protocols from two previous works (Dehaut et al., 2016; Karami et al., 2017a). Samples were weighed and placed in a glass container. A 10% KOH solution was prepared using 1.6 μm-filtered deionised water and KOH tablets (Sigma-Aldrich). This solution was added to each jar in a ratio with the sample of 1:8 (w/v). The containers were then sealed and incubated at room temperature for 7 days. To prevent plastic contamination, cotton laboratory coats, face masks and single-use latex gloves were worn during sample handling, preparation of samples and during the entire experiment. Work surfaces were thoroughly washed with 70% ethanol prior starting all procedures. All liquids (deionised water for cleaning and for preparation of KOH solution) were filtered through 1.6 μm-pore-size filter membrane (Whatman GF/A). Glassware and instruments, including scissors, tweezers and scalpels, were washed using dishwashing liquid, rinsed with deionised water and finally rinsed with 1.6 μm-filtered deionised water. Since the experiments were conducted without the use of the laminar flow hood, the plastic fibres found in the samples were not considered in the results. Digestates were then filtered through 1.6 μm-pore-size filter membrane (Whatman GF/A) using a vacuum pump connected to a filter funnel. The filter papers were dried at room temperature and stored in glass Petri dishes until visual identification and spectroscopic characterization of plastic particles. Three procedural blanks, obtained following the same procedure above described, but without placenta samples and maintained close to the samples during their manipulation, were tested to monitor and correct potential contaminations (Karami et al., 2017a).

2.4. Analysis of microplastics by Raman Microspectroscopy

The Raman analysis of MPs was performed at the Laboratory of Vibrational Spectroscopy, Department of Life and Environmental Sciences, Università Politecnica delle Marche (Ancona, Italy). Filter membranes were first inspected by visible light using a ×10 objective (Olympus MPLAN10x/0.25). The detected MPs were morphologically characterized by a ×100 objective (Olympus MPLAN100x/0.90), and then directly analyzed on the filter by Raman Microspectroscopy (spectral range 160–2000 cm^{-1}, 785 nm laser diode, 600 lines per mm grating). A Raman XploRA Nano Microspectrometer (Horiba Scientific) was used. The spectra were dispersed onto a 16-bit dynamic range Peltier cooled CCD detector; the spectrometer was calibrated to the 520.7 cm^{-1} line of silicon prior to spectral acquisition. Raw Raman spectra were submitted to polynomial baseline correction and vector normalization, in order to reduce noise and enhance spectrum quality (Labspec 6 software, Horiba Scientific). The collected Raman spectra were compared with those reported in the SLOPP Library of Microplastics ("SLOPP Library of Microplastics," n.d.) and in the spectral library of the KnowItAll software (Bio-Rad Laboratories, Inc.). Similarities of more than 80 of Hit Quality Index (HQI) were considered satisfactory.

3. Results

From each placenta, three portions with a mean weight of 23.3 ± 5.7 g were collected from the maternal side, the foetal side and the chorioamniotic membranes. All portions were opportunely processed for the subsequent analysis by Raman Microspectroscopy.

In total, 12 MP fragments (named #1–#12) were detected in the placentas of four women; more in detail, 5 MPs were found in the foetal side portions, 4 in the maternal side portions, and 3 in the chorioamniotic membranes. Microplastics #1–#4, #6, #7, and #9–#12, were ~10 μm in size, while #5 and #8 ones were smaller (~5 μm). All the analyzed MPs were pigmented.

A retrospective analysis based on Raman spectral information and data reported in literature was performed to define the nature of these MPs. Firstly, the collected Raman spectra were compared with those stored in the spectral library of the KnowItAll software (Bio-Rad Laboratories, Inc.). In many cases, the collected Raman spectra showed, above all, the contribution of the pigments used for plastic staining (Imhof et al., 2016; Stoye and Freitag, 1998); it is known that the conjugated rings present in pigment molecules are highly polarizable and, hence, their Raman signals are more intense than those of the apolar polymeric matrix (Käppler et al., 2016). In these cases, the KnowItAll software identified the pigments contained in the MPs. By matching the results from the KnowItAll software with the information obtained by consulting the European Chemical Agency, ECHA ("European Chemical Agency," n.d.), it was possible to accurately identify the commercial name, chemical formula, IUPAC name and Color Index Constitution Number of all pigments. Further, in order to uncover the identity of the polymer matrix of the detected MPs, the collected Raman spectra were also compared with those reported in the SLOPP library of Microplastics.

The identified MPs were differentiated between stained MPs (particles #2, #10 and #11, identified as polypropylene) and paint/coating/dye MPs (particles #1, #3–9, and #12), which are applied for paints, coatings, adhesives, plasters, polymers and cosmetics and personal care products (Imhof et al., 2016).

The microphotographs and the Raman spectra of all analysed MPs are shown in Fig. 2, while Table 1 reports their morphological and chemical characterization. The spectral analysis is reported below.

Particle #1 (Fig. 2a): the Raman spectrum resulted superimposable to the one of the pigment Iron hydroxide oxide yellow (main peak at 396 cm^{-1}, related to the vibrations of iron oxides/hydroxides) (Sklute et al., 2018).

Particles #2, #5, and #10 (Fig. 2b, e): the Raman spectra resulted comparable to the one of a polypropylene (PP) blue sample, sharing the main peaks at 253 cm^{-1} (wagging of CH$_2$ moieties, bending of CH moieties), 397 cm^{-1} (wagging of CH$_2$ moieties, bending of CH moieties), 839 cm^{-1} (rocking of CH$_2$ and CH$_3$ moieties, stretching of CC and C-CH$_3$ moieties), 970 cm^{-1} (rocking of CH$_3$ moieties), and 1455 cm^{-1} (bending of CH$_3$ and CH$_2$ moieties), all assigned to PP (Andreassen, 1999). The bands at 679 cm^{-1}, 1143 cm^{-1}, 1340 cm^{-1} and 1527 cm^{-1}, common to reference blue polypropylene and sample spectra, are known to be related to Raman signals of blue pigments, mainly based on copper phthalocyanine (Aguayo et al., 2010; Scherrer et al., 2009).

Particle #3 (Fig. 2c): the Raman spectrum resulted superimposable to the one of the blue pigment phthalocyanine, sharing the main peaks at 679 cm^{-1}, 1143 cm^{-1}, 1340 cm^{-1} and 1527 cm^{-1} (Aguayo et al., 2010; Scherrer et al., 2009).

Particle #4 (Fig. 2d): the Raman spectrum resulted superimposable to the one of the pigment violanthrone, with the two main peaks centered at 1577 cm^{-1} (C-C stretching of benzene ring) and 1307 cm^{-1} (in reference spectrum, an additional shoulder at ~1350 cm^{-1} is visible, assigned to C-C stretching and HC-C bending) (Socrates, 2001).

Particles #6 and #7 (Fig. 2f): the Raman spectra resulted superimposable to the one of the red pigment oxo(oxoferriooxy)iron (main peaks at 220, 287 and 401 cm^{-1}, typical of iron oxides) (Testa-Anta et al., 2019).
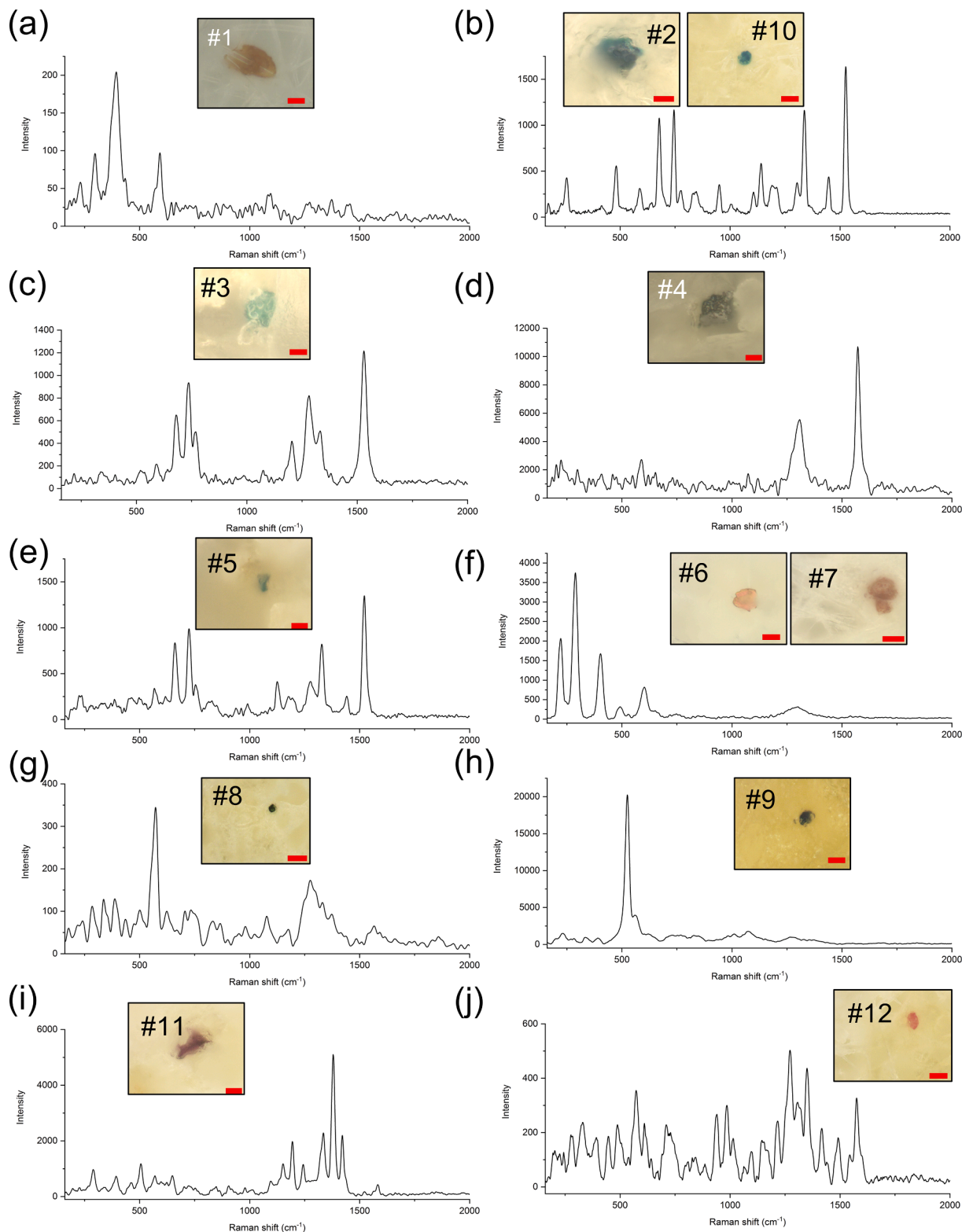
Fig. 2. Microphotographs and Raman spectra of the microplastics found in human placenta: (a) Particle #1 (scale bar 5 μm); (b) Particles #2 and #10 (scale bar 5 μm for #2 and 10 μm for #10); (c) Particle #3 (scale bar 5 μm); (d) Particle #4 (scale bar 5 μm); (e) Particle #5 (scale bar 5 μm); (f) Particles #6 and #7 (scale bar 10 μm for #6 and 5 μm for #7); (g) Particle #8 (scale bar 10 μm); (h) Particle #9 (scale bar 10 μm); (i) Particle #11 (scale bar 5 μm), and (l) Particle #12 (scale bar 10 μm).

Particle #8 (Fig. 2g): the Raman spectrum resulted superimposable to the one of the pigment Direct Blue 80, showing two main peaks at 578 cm^{-1} and 1275 cm^{-1} (both assigned to ring deformations of substituted benzene) (Socrates, 2001).

Particle #9 (Fig. 2h): the Raman spectrum resulted superimposable

to the one of the pigment Ultramarine Blue, with one main peak centred at 525 cm^{-1}, assigne to orthosilicate vibration modes (Socrates, 2001).

Particle #11 (Fig. 2i): the Raman spectrum resulted comparable to the one of a PP purple fiber, sharing the main peaks of PP (Andreassen, 1999) (397 cm^{-1}, assigned to the wagging of CH$_2$ moieties/bending of

Table 1

Size, color and chemical features of the detected microplastics and relative pigments, together with information regarding the placenta portion in which they were found (fetal side FS; maternal side MS, and chorioamnio membrane CAM; not defined n.d.; Hit Quality Index HQI).

Particle	Placenta Portion	Microparticles					
		Size	Color	Polymer matrix	Pigment		
					Generic name	Molecular formula and IUPAC name	HQI
#1	FS	~10 μm	Orange	n.d.	Iron hydroxide oxide yellow (Pigment Yellow 43; C.I. Constitution 77492)	FeO(OH) iron(III) oxide hydroxide	89.97
#2	CAM	~10 μm	Blue	Polypropylene	Copper phthalocyanine (Pigment Blue 15; C.I. Constitution 74160)	$C_{32}H_{16}CuN_8$ (29H,31H-phthalocyaninato(2 −)-N29,N30,N31,N32)copper(II)	82.86
#3	FS	~10 μm	Blue	n.d.	Phthalocyanine Blue BN (Pigment Blue 16; C.I. Constitution 74100)	$C_{32}H_{18}N_8$29H,31H-phthalocyanine	89.16
#4	MS	~10 μm	Dark blue	n.d.	Violanthrone (Pigment Blue 65; C. I. Constitution 59800)	$C_{34}H_{16}O_2$Anthra[9,1,2-cde]benzo[rst]pentaphene-5,10-dione	86.44
#5	MS	~5 μm	Blue	Polypropylene	Copper phthalocyanine (Pigment Blue 15; C.I. Constitution 74160)	$C_{32}H_{16}CuN_8$ (29H,31H-phthalocyaninato(2−)-N29,N30,N31,N32)copper(II)	86.15
#6	MS	~10 μm	Red	n.d.	Diiron trioxide (Pigment Red 101/102; C.I. Constitution 77491)	Fe_2O_3 Oxo(oxoferriooxy)iron	83.65
#7	MS	~10 μm	Red	n.d.	Diiron trioxide (Pigment Red 101/102; C.I. Constitution 77491)	Fe_2O_3Oxo(oxoferriooxy)iron	89.80
#8	CAM	~5 μm	Dark blue	n.d.	Pigment Direct Blue 80	$C_{32}H_{14}Cu_2N_4Na_4O_{16}S_4$ Dicopper,tetrasodium,3-oxido-4-[[2-oxido-4-[3-oxido-4-[(2-oxido-3,6-disulfonatonaphthalen-1-yl)diazenyl] phenyl]phenyl] diazenyl]naphthalene-2,7-disulfonate	84.55
#9	CAM	~10 μm	Dark blue	n.d.	Ultramarine Blue (Pigment Blue 29; C.I. Constitution 77007)	$Al_6Na_8O_{24}S_3Si_6$ Aluminium Sodium orthosilicate trisulfane-1,3-diide	91.96
#10	FS	~10 μm	Blue	Polypropylene	Copper phthalocyanine (Pigment Blue 15; C.I. Constitution 74160)	$C_{32}H_{16}CuN_8$ (29H,31H-phthalocyaninato(2−)-N29,N30,N31,N32)copper(II)	80.60
#11	FS	~10 μm	Violet	Polypropylene	Hostopen violet (Pigment Violet 23; C.I. Constitution 51319)	$C_{34}H_{22}Cl_2N_4O_2$ 8,18-Dichloro-5,15-diethyl-5,15-dihydrodiindolo(3,2-b:3′,2′-m) tri- phenodioxazine	80.92
#12	FS	~10 μm	Pink	n.d.	Novoperm Bordeaux HF3R (Pigment Violet 32; C.I. Constitution 12517)	$C_{27}H_{24}N_6O_7S$ 4-[(E)-2-[2,5-dimethoxy-4-(methylsulfamoyl)phenyl]diazen-1-yl]-3-hydroxy-N-(2-oxo-2,3-dihydro-1H-1,3-benzodiazol-5-yl) naphthalene-2-carboxamide	84.57

CH moieties, and 1455 cm^{-1}, assigned to the bending of CH$_3$ and CH$_2$ moieties), and also of the violet pigment (1193 cm^{-1}, 1335 cm^{-1} and 1381 cm^{-1}) (Scherrer et al., 2009).

Particle #12 (Fig. 2j): the collected Raman spectrum resulted superimposable to the one of the pink pigment Novoperm Bordeaux HF3R. The Raman spectrum of this monoazopigment shared with the sample spectrum the main peaks centered at 731 cm^{-1}, 961 cm^{-1}, 1219 cm^{-1}, 1280 cm^{-1}, 1360 cm^{-1}, and 1580 cm^{-1}. This pigment is reported to be used to permanently coat and protect wood surfaces, in photographic chemicals, inks and toners, given its high solvent resistance and good heat stability (Scherrer et al., 2009).

4. Discussion

This is the first study revealing the presence of pigmented microplastics and, in general, of man-made particles in human placenta. The presence of pigments in all analysed MPs is explained by the wide use of these compounds to colour not only plastic products, but also paints and coatings, which are as ubiquitous as MPs (Imhof et al., 2016). For example, the pigment Iron hydroxide oxide yellow (particle #1) is used for coloration of polymers (plastics and rubber) and in a wide variety of cosmetics, such as BB creams and foundations; copper phthalocyanine (particles #2, #5, #10,) and phthalocyanine (particle #3) are used for staining of plastic materials (polyvinylchloride, low density polyethylene, high density polyethylene, polypropylene, polyethylene terephthalate), and for finger paints; the pigment violanthrone (particle #4) is used especially for textile (cotton/polyester) dyeing, coating products, adhesives, fragrances and air fresheners; the pigment Ultramarine blue is mainly applied in cosmetics, for example for formulations of soap, lipstick, mascara, eye shadow and other make-up products.

For the first time, by means of Raman Microspectroscopy, 12 MP fragments were isolated in four human placentas. In particular, 5 MPs were found in the foetal side, 4 in the maternal side and 3 in the chorioamniotic membranes, indicating that these MPs, once inside the human body, can reach placenta tissues at all levels. It is noteworthy to remark that small portions of placentas (~23 g with respect to a total weight of ~600 g) were analysed, letting hypothesize that the number of MPs within the entire placenta is much higher.

The dimensions of all MPs were ~10 μm in size, except for two that were smaller (~5 μm). These values are compatible with a possible transportation by bloodstream. In fact, previous analyses performed by means of Electron Microscopy coupled with an X-ray microprobe, revealed the presence of 5–10 μm particles as foreign bodies in human internal organs (Vaseashta, 2015).

Unfortunately, we do not know how MPs reach the bloodstream and if they come from the respiratory system or the gastrointestinal system. Fig. 3 shows the possible ways of entry and transport of the MPs from the respiratory and gastric organs to the placenta.

The presence of MPs in the placenta tissue requires the reconsideration of the immunological mechanism of self-tolerance. Placenta represents the interface between the foetus and the environment (PrabhuDas et al., 2015). Embryos and foetuses must continuously adapt to the maternal environment and, indirectly, to the external one, by a series of complex responses. An important part of this series of responses consists in the ability to differentiate self and non-self (Nancy et al., 2012), a mechanism that may be perturbed by the presence of MPs. In fact, it is reported that, once present in the human body, MPs may accumulate and exert localized toxicity by inducing and/or enhancing immune responses and, hence, potentially reducing the defence mechanisms against pathogens and altering the utilization of energy stores (Wright and Kelly, 2017).

Microplastics may access the bloodstream and reach placenta from the maternal respiratory system (Schlesinger, 1988) and the gastrointestinal tract (GIT) (Arumugasaamy et al., 2019), by means of M cells-
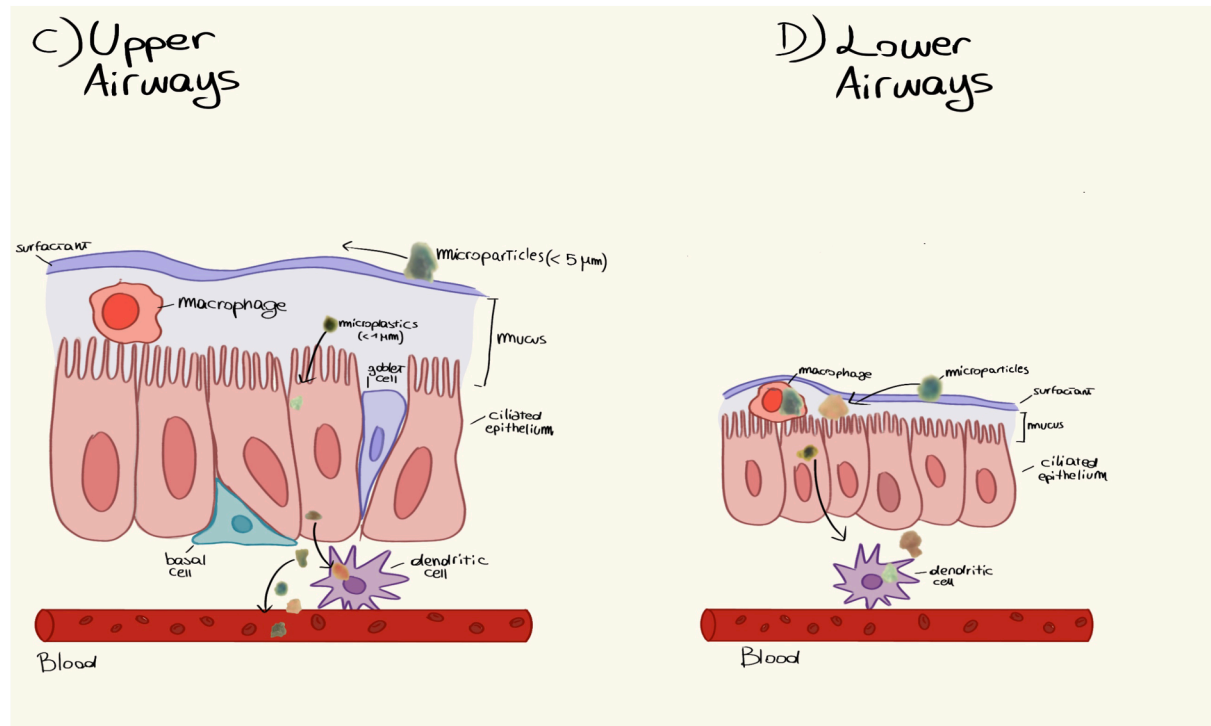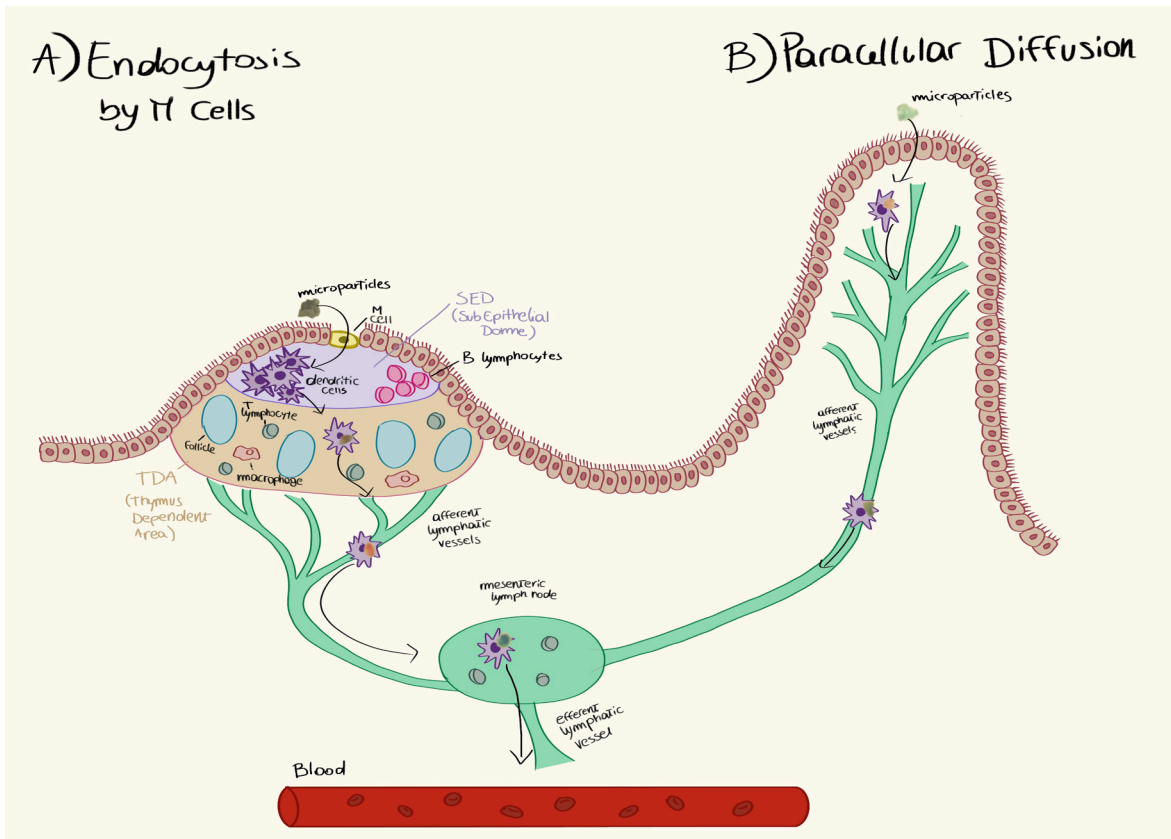
(caption on next page)

Fig. 3. A-B-C-D. Hypothetical mechanisms by which microplastics penetrate human tissues. (A) Endocytosis by M cells. At the level of the Peyer's Patched, below the mucous gut, MPs ingested with food can be uptaken by endocytosis from the M cells, transported across the epithelium into the subepithelial dome where they encounter dendritic cells, which in turn transport them through the lymphatic circulation, from where they reach the blood. (B) Paracellular Diffusion. MPs could penetrate through the intestinal lumen from loose junctions. This phenomenon could partially explain why some inflammatory states, which increase loose junctions favour intestinal passage. Once the intestinal lumen has been crossed, the MPs are collected by the dendritic cells and transported in the lymphatic and subsequently in the systemic circulation. (C) Upper airways, At the level of the upper respiratory tract the mucus is thicker and allows a successful clearance of the foreign bodies particles, in addition, the mechanical movement of ciliated epithelium and the presence of surfactant prevents smaller particles from spreading through the epithelium and reach the circulation. (D) Lower airways, In the lower respiratory tract the mucus layer is thinner, thus facilitating the diffusion of particles which, thanks to their particular aerodynamic shape, are able to reach this part of the respiratory tract. Once penetrated, the MPs can spread into the general circulation by cellular uptake or diffusion. (*Modified from: Mowat, A. Anatomical basis of tolerance and immunity to intestinal antigens. Nat Rev Immunol **3**, 331–341 (2003). https://doi.org/10.1038/nri1057. And Ruge, C. A.; Kirch, J.; Lehr, C. M. Pulmonary drug delivery: From generating aerosols to overcoming biological barriers-therapeutic possibilities and technological challenges. Lancet. Respir. Med. 2013, 1(5), 402–413.)*

mediated endocytosis mechanisms or paracellular transport. The most probable transport route for MPs is a mechanism of particle uptake and translocation, already described for the internalization from the GIT (Smith et al., 2018). The subsequent translocation to secondary target organs, usually associated with inflammatory responses in the surrounding tissues, such as the immune activation of macrophages and the production of cytokines (Hicks et al., 1996), depends on several factors, including hydrophobicity, surface charge, surface functionalization and the associated protein corona, and particle size.

Once MPs have reached the maternal surface of the placenta, as other exogenous materials, they can invade the tissue in depth by several transport mechanisms, both active and passive, that are not clearly understood yet (Tetro et al., 2018). The transplacental passage of 5–10 μm size MPs may depend on different physiological conditions and genetic characteristics. This might explain, together with the diverse food habits and lifestyle of patients, the absence of MPs in 2 of the 6 analyzed placentas and the different localization and characteristics of the particles identified in the present study. It is known that a great variability exists in the expression and function of placental drug transporters, both within human populations (inter-individual variability) and also during gestation (intra-individual variability) (Staud and Ceckova, 2015). We suppose that this variability exists also in relation to the mechanism of particles' internalization.

Potentially, MPs, and in general microparticles, may alter several cellular regulating pathways in placenta, such as immunity mechanisms during pregnancy, growth-factor signalling during and after implantation, functions of atypical chemokine receptors governing maternal-foetal communication, signalling between the embryo and the uterus, and trafficking of uterine dendritic cells, natural killer cells, T cells and macrophages during normal pregnancy. All these effects may lead to adverse pregnancy outcomes including preeclampsia and fetal growth restriction (Ilekis et al., 2016).

In conclusion, this study sheds new light on the level of human exposure to MPs and microparticles in general. Due to the crucial role of placenta in supporting the foetus development and in acting as an interface between the latter and the external environment, the presence of exogenous and potentially harmful (plastic) particles is a matter of great concern. Possible consequences on pregnancy outcomes and foetus are the transgenerational effects of plasticizer on metabolism and reproduction (Lee, 2018). Further studies need to be performed to assess if the presence of MPs in human placenta may trigger immune responses or may lead to the release of toxic contaminants, resulting harmful for pregnancy.

Declaration of Competing Interest

The authors declare that they have no known competing financial interests or personal relationships that could have appeared to influence the work reported in this paper.

References

Aguayo, T., Clavijo, E., Villagràn, A., Espinosa, F., Sagues, F.E., Campos-Vallette, M., 2010. Raman vibrational study of pigments with patrimonial interest for the Chilean cultural heritage. J. Chil. Chem. Soc. 55, 347–351. https://doi.org/10.4067/S0717-97072010000300016.

Andreassen, E., 1999. Infrared and Raman spectroscopy of polypropylene. In: Karger-Kocsis, J. (Ed.), Polypropylene: An A-Z Reference. Kluwer Publishers, Dordrecht, Dordrecht. https://doi.org/10.1007/978-94-011-4421-6.

Arumugasaamy, N., Navarro, J., Kent Leach, J., Kim, P.C.W., Fisher, J.P., 2019. In vitro models for studying transport across epithelial tissue barriers. Ann. Biomed. Eng. 47, 1–21. https://doi.org/10.1007/s10439-018-02124-w.

Barboza, L.G.A., Dick Vethaak, A., Lavorante, B.R.B.O., Lundebye, A.-K., Guilhermino, L., 2018. Marine microplastic debris: An emerging issue for food security, food safety and human health. Mar. Pollut. Bull. 133, 336–348. https://doi.org/10.1016/j.marpolbul.2018.05.047.

de Souza Machado, A.A., Kloas, W., Zarfl, C., Hempel, S., Rillig, M.C., 2018. Microplastics as an emerging threat to terrestrial ecosystems. Glob. Chang. Biol. 24, 1405–1416. https://doi.org/10.1111/gcb.14020.

Dehaut, A., Cassone, A.-L., Frère, L., Hermabessiere, L., Himber, C., Rinnert, E., Rivière, G., Lambert, C., Soudant, P., Huvet, A., Duflos, G., Paul-Pont, I., 2016. Microplastics in seafood: Benchmark protocol for their extraction and characterization. Environ. Pollut. 215, 223–233. https://doi.org/10.1016/j.envpol.2016.05.018.

Deng, Y., Zhang, Y., Lemos, B., Ren, H., 2017. Tissue accumulation of microplastics in mice and biomarker responses suggest widespread health risks of exposure. Sci. Rep. 7, 46687. https://doi.org/10.1038/srep46687.

EFSA Panel on Contaminants in the Food Chain (CONTAM), 2016. Presence of microplastics and nanoplastics in food, with particular focus on seafood. EFSA J. 14, 4501–4531. https://doi.org/10.2903/j.efsa.2016.4501.

European Chemical Agency [WWW Document], n.d. URL https://echa.europa.eu.

Hartmann, N.B., Hüffer, T., Thompson, R.C., Hassellöv, M., Verschoor, A., Daugaard, A. E., Rist, S., Karlsson, T., Brennholt, N., Cole, M., Herrling, M.P., Hess, M.C., Ivleva, N. P., Lusher, A.L., Wagner, M., 2019. Are we speaking the same language? Recommendations for a definition and categorization framework for plastic debris. Environ. Sci. Technol. 53, 1039–1047. https://doi.org/10.1021/acs.est.8b05297.

D.G. Hicks A.R. Judkins J.Z. Sickel R.N. Rosier J.E. Puzas R.J. O'Keefe Granular histiocytosis of pelvic lymph nodes following total hip arthroplasty. The presence of wear debris, cytokine production, and immunologically activated macrophages* J. Bone Jt. Surg. 78 1996 482 96 10.2106/00004623-199604000-00002.

Ilekis, J.V., Tsilou, E., Fisher, S., Abrahams, V.M., Soares, M.J., Cross, J.C., Zamudio, S., Illsley, N.P., Myatt, L., Colvis, C., Costantine, M.M., Haas, D.M., Sadovsky, Y., Weiner, C., Rytting, E., Bidwell, G., 2016. Placental origins of adverse pregnancy outcomes: potential molecular targets: an Executive Workshop Summary of the Eunice Kennedy Shriver National Institute of Child Health and Human Development. Am. J. Obstet. Gynecol. 215, S1–S46. https://doi.org/10.1016/j.ajog.2016.03.001.

Imhof, H.K., Laforsch, C., Wiesheu, A.C., Schmid, J., Anger, P.M., Niessner, R., Ivleva, N. P., 2016. Pigments and plastic in limnetic ecosystems: A qualitative and quantitative study on microparticles of different size classes. Water Res. 98, 64–74. https://doi.org/10.1016/j.watres.2016.03.015.

Käppler, A., Fischer, D., Oberbeckmann, S., Schernewski, G., Labrenz, M., Eichhorn, K.-J., Voit, B., 2016. Analysis of environmental microplastics by vibrational microspectroscopy: FTIR, Raman or both? Anal. Bioanal. Chem. 408, 8377–8391. https://doi.org/10.1007/s00216-016-9956-3.

Karami, A., Golieskardi, A., Choo, C.K., Romano, N., Ho, Y. Bin, Salamatinia, B., 2017a. A high-performance protocol for extraction of microplastics in fish. Sci. Total Environ. 578, 485–494. https://doi.org/10.1016/j.scitotenv.2016.10.213.

Karami, A., Golieskardi, A., Keong Choo, C., Larat, V., Galloway, T.S., Salamatinia, B., 2017b. The presence of microplastics in commercial salts from different countries. Sci. Rep. 7, 46173. https://doi.org/10.1038/srep46173.

Kosuth, M., Mason, S.A., Wattenberg, E.V., 2018. Anthropogenic contamination of tap water, beer, and sea salt. PLoS One 13, e0194970. https://doi.org/10.1371/journal.pone.0194970.

Lee, D.-H., 2018. Evidence of the possible harm of endocrine-disrupting chemicals in humans: ongoing debates and key issues. Endocrinol. Metab. 33, 44. https://doi.org/10.3803/EnM.2018.33.1.44.

Nancy, P., Tagliani, E., Tay, C.-S., Asp, P., Levy, D.E., Erlebacher, A., 2012. Chemokine gene silencing in decidual stromal cells limits T Cell access to the maternal-fetal interface. Science (80-.) 336, 1317–1321. https://doi.org/10.1126/science.1220030.

Notarstefano, V., Gioacchini, G., Byrne, H.J., Zacà, C., Sereni, E., Vaccari, L., Borini, A., Carnevali, O., Giorgini, E., 2019. Vibrational characterization of granulosa cells from patients affected by unilateral ovarian endometriosis: New insights from infrared and Raman microspectroscopy. Spectrochim. Acta Part A Mol Biomol. Spectrosc. 212, 206–214. https://doi.org/10.1016/j.saa.2018.12.054.

Notarstefano, V., Sabbatini, S., Pro, C., Belloni, A., Orilisi, G., Rubini, C., Byrne, H.J., Vaccari, L., Giorgini, E., 2020. Exploiting Fourier Transform InfraRed and Raman microspectroscopies on Cancer Stem Cells from Oral Squamous Cells Carcinoma: new evidence of acquired cisplatin chemoresistance. Analyst. https://doi.org/10.1039/D0AN01623C.

PlasticsEurope, 2016. Plastics – the Facts 2016 An analysis of European plastics production, demand and waste data [WWW Document]. URL https://www.plasticseurope.org/application/files/4315/1310/4805/plastic-the-fact-2016.pdf.

PrabhuDas, M., Bonney, E., Caron, K., Dey, S., Erlebacher, A., Fazleabas, A., Fisher, S., Golos, T., Matzuk, M., McCune, J.M., Mor, G., Schulz, L., Soares, M., Spencer, T., Strominger, J., Way, S.S., Yoshinaga, K., 2015. Immune mechanisms at the maternal-fetal interface: perspectives and challenges. Nat. Immunol. 16, 328–334. https://doi.org/10.1038/ni.3131.

Reineke, J.J., Cho, D.Y., Dingle, Y.-T., Morello, A.P., Jacob, J., Thanos, C.G., Mathiowitz, E., 2013. Unique insights into the intestinal absorption, transit, and subsequent biodistribution of polymer-derived microspheres. Proc. Natl. Acad. Sci. 110, 13803–13808. https://doi.org/10.1073/pnas.1305882110.

Ribeiro-Claro, P., Nolasco, M.M., Araújo, C., 2017. Characterization of microplastics by Raman spectroscopy. Compr. Anal. Chem. 75, 119–151. https://doi.org/10.1016/bs.coac.2016.10.001.

Scherrer, N.C., Stefan, Z., Francoise, D., Annette, F., Renate, K., 2009. Synthetic organic pigments of the 20th and 21st century relevant to artist's paints: Raman spectra

reference collection. Spectrochim Acta Part A Mol. Biomol. Spectrosc. 73, 505–524. https://doi.org/10.1016/j.saa.2008.11.029.

Schlesinger, R.B., 1988. Biological disposition of airborne particles: basic principles and application to vehicular emissions. In: Watson, A.Y., Bates, R.R., Kennedy, D. (Eds.), Air Pollution, the Automobile, and Public Health.

Schwabl, P., Köppel, S., Königshofer, P., Bucsics, T., Trauner, M., Reiberger, T., Liebmann, B., 2019. Detection of various microplastics in human stool. Ann. Intern. Med. 171, 453. https://doi.org/10.7326/M19-0618.

Schymanski, D., Goldbeck, C., Humpf, H.-U., Fürst, P., 2018. Analysis of microplastics in water by micro-Raman spectroscopy: Release of plastic particles from different packaging into mineral water. Water Res. 129, 154–162. https://doi.org/10.1016/j.watres.2017.11.011.

Sklute, E.C., Kashyap, S., Dyar, M.D., Holden, J.F., Tague, T., Wang, P., Jaret, S.J., 2018. Spectral and morphological characteristics of synthetic nanophase iron (oxyhydr) oxides. Phys. Chem. Miner. 45, 1–26. https://doi.org/10.1007/s00269-017-0897-y.

SLOPP Library of Microplastics [WWW Document], n.d. URL https://rochmanlab.com/slopp-and-slopp-e-raman-spectral-libraries-for-microplastics-research.

Smith, D.J., Leal, L.G., Mitragotri, S., Shell, M.S., 2018. Nanoparticle transport across model cellular membranes: when do solubility-diffusion models break down? J. Phys. D. Appl. Phys. 51, 294004. https://doi.org/10.1088/1361-6463/aacac9.

Socrates, G., 2001. Infrared and Raman Characteristic Group Frequencies. Tables and chartsGeorge Socrates John Wiley and Sons, Ltd, Chichester, third ed., 2001. Price £135. John Wiley & Sons, Ltd. https://doi.org/10.1002/jrs.1238.

Staud, F., Ceckova, M., 2015. Regulation of drug transporter expression and function in the placenta. Expert Opin. Drug Metab. Toxicol. 11, 533–555. https://doi.org/10.1517/17425255.2015.1005073.

Stoye, D., Freitag, W. (Eds.), 1998. Paints, Coatings and Solvents. Wiley. https://doi.org/10.1002/9783527611867.

Testa-Anta, M., Ramos-Docampo, M.A., Comesaña-Hermo, M., Rivas-Murias, B., Salgueiriño, V., 2019. Raman spectroscopy to unravel the magnetic properties of iron oxide nanocrystals for bio-related applications. Nanoscale Adv. 1, 2086–2103. https://doi.org/10.1039/C9NA00064J.

Tetro, N., Moushaev, S., Rubinchik-Stern, M., Eyal, S., 2018. The placental barrier: the gate and the fate in drug distribution. Pharm. Res. 35, 71. https://doi.org/10.1007/s11095-017-2286-0.

Vaseashta, A. (Ed.), 2015. Life Cycle Analysis of Nanoparticles: risk, assessment, and sustainability. DEStech Publications, Inc.

Wright, S.L., Kelly, F.J., 2017. Plastic and Human Health: A Micro Issue? Environ. Sci. Technol. 51, 6634–6647. https://doi.org/10.1021/acs.est.7b00423.